

AN ALTERNATIVE FLUID DYNAMIC EXPLANATION FOR PROPULSION IN FRONT CRAWL SWIMMING

Huub M. Toussaint

Institute for Fundamental and Clinical Human Movement Science,
Vrije Universiteit, van der Boechortsstraat 9, 1081 BT Amsterdam,
The Netherlands

Calculation of propulsion in front crawl swimming relies on the quasi-steady assumption that the fluid dynamic behaviour of a hand model in a flow channel (constant velocity and orientation) is similar to that of a hand of a real swimmer swimming the front crawl. It has been shown that quasi-steady calculations cannot account for the observed propulsive forces during front crawl swimming. Using woollen tufts the flow pattern around the arm and hand during the front crawl stroke was visualised. The flow direction varied strongly throughout the stroke and a strong, accelerating axial flow, not in the direction of the arm movement, was observed. These observations discredit the quasi-steady analysis of front crawl swimming. Instead, it is proposed that rotation of the arm leads to a proximo-distal pressure gradient, inducing axial flow. Such axial flow along the trailing side of the arm could greatly enhance the pressure difference over the hand, thus assisting propulsion by paddling.

KEY WORDS: fluid dynamics, propulsion, front crawl swimming, quasi-steady analysis, arm rotation, axial flow

INTRODUCTION: Propulsion is one of the key factors determining performance in human competitive swimming. James Counsilman was one of the first to apply physical principles to try to understand the mechanism of propulsion (Berg & Ellington, 1997a; Berg & Ellington, 1997b; Ellington et al., 1996). Originally, he proposed that the hand is used as an oar pushing water straight backwards. In other words, propulsion would be generated entirely by drag forces. However, close inspection of underwater movies of skilled swimmers revealed sculling hand motions rather than straight backward pulls. If propulsion was based purely on drag forces, such sculling movements would be wasteful. Counsilman reasoned that the observed complex hand patterns would be compatible with the generation of efficient propulsion (i.e. directed straight forward) if the hand acts as a hydrofoil generating both lift and drag forces (Berg & Ellington, 1997a; Berg & Ellington, 1997b; Ellington et al., 1996). In general, when an object is moved through a fluid, the net force acting upon it may be split into two perpendicular components: the drag force D acting opposite to the direction of movement and the lift force L acting perpendicular to the direction of relative movement. The magnitude of the lift force depends on the shape of the object and its orientation with respect to the flow. The fluid dynamic forces acting on an object are usually described as a function of its velocity relative to the fluid (u , $m \cdot s^{-1}$), its surface area (plan area S , m^2) and the density of the fluid ρ , $kg \cdot m^{-3}$) according to

$$L = \frac{1}{2} \rho u^2 C_l S \quad (2)$$

$$D = \frac{1}{2} \rho u^2 C_d S \quad (2)$$

where C_l and C_d are the lift and drag coefficients, respectively.

To further explore Counsilman's suggestion, Schleihau (Berg & Ellington, 1997a; Berg & Ellington, 1997b; Ellington et al., 1996) investigated the hydrofoil behaviour of an exact plastic resin replica of the hand in a flow channel through which fluid flowed at a constant speed. The C_l and C_d values reported by Schleihau showed that lift forces might indeed play a significant role in propulsion. The next step, therefore, was to combine the flow channel data with hand velocity data collected from film analysis of leading swimmers. Using equation 1 and 2 the magnitude and direction of the resultant of the lift and drag force acting on the

hand throughout the stroke cycle was calculated (Berg & Ellington, 1997a; Berg & Ellington, 1997b; Ellington et al., 1996). These calculations corroborated Counsilman's hypothesis that both lift and drag forces are generated during the stroke and that the resultant force is predominantly directed forward. It is important to note that Schleihauf's analysis of the swimming stroke is quasi-steady, i.e. it crucially depends on the assumption that the flow under steady conditions (constant velocity, constant angle of attack and sweep back angle) in the flow channel is comparable to the flow during the actual swimming stroke.

Recently some doubt was cast whether the quasi-steady analysis can account quantitatively for high propulsive forces required for high-speed swimming. When swimming at a constant speed the average propulsive force should equal the average resistive force. A comparison was made between the propulsive forces calculated using Schleihauf's approach and those measured on the M.A.D.-system (system to Measure Active Drag). With this device the propulsive forces generated by swimmers pushing off from fixed points along the swimming track were measured directly (Berg & Ellington, 1997a; Berg & Ellington, 1997b; Ellington et al., 1996). Berger et al. (Berg & Ellington, 1997a; Berg & Ellington, 1997b; Ellington et al., 1996) calculated quasi-steady forces that were considerably lower (17%) than the measured propulsive forces (M.A.D.-system), when the hand velocity was set approximately equal to the velocity of the middle of the palm of the hand, i.e. the hand's aerodynamic centre according to Schleihauf (Berg & Ellington, 1997a; Berg & Ellington, 1997b; Ellington et al., 1996).

How can the observed discrepancy be accounted for? It seems reasonable to question the validity of the quasi-steady assumption for front crawl swimming. And, if this assumption indeed proves to be not valid, how else might we attempt to approach the problem?

Given this question it is interesting to make a side step to the fluid dynamics of insect flight, which was faced with a similar crisis some time ago (Berg & Ellington, 1997a; Berg & Ellington, 1997b; Ellington et al., 1996). Insect flight was analysed using the quasi-steady approach, equivalent to Schleihauf's work, which provided a satisfactory account of fast forward flight (Berg & Ellington, 1997a; Berg & Ellington, 1997b; Ellington et al., 1996). However, a number of observations led to gradual erosion of the confidence in the applicability of the quasi-steady assumption.

One way to look at the total fluid flow around a (hydro)foil is to decompose it in a circulating flow around the hydrofoil with velocity (v) and an uniform flow field at velocity (u) (Figure 1). Note that the fluid particles do not actually circle around the hydrofoil; rather, the flow-pattern can be thought of as a superposition of translation and circulation as indicated in Figure 1.

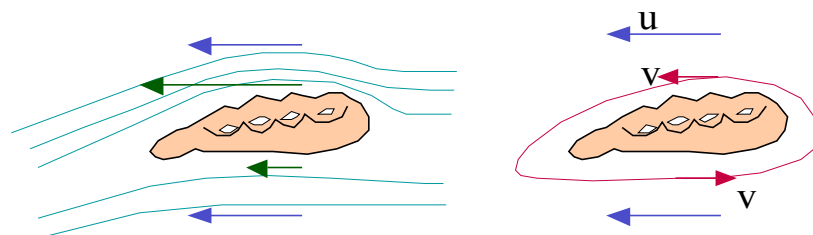


Figure 1 - Streamlines around a hand-hydrofoil in a flow from right to left. The flow past the hand can be decomposed in a uniform flow field with velocity u and a circulating flow around the hydrofoil with velocity v . The circulating flow is known as the *Bound Vortex*.

The circulating flow component is known as the *bound vortex* (Berg & Ellington, 1997a; Berg & Ellington, 1997b; Ellington et al., 1996). The higher the circulation, the greater the velocity differential above and below the hand with, according to Bernoulli's equation, a concomitant greater pressure differential and thus higher lift force.

When a hydrofoil is accelerated impulsively to a constant velocity, the bound vortex needs time to develop to its final, steady-state strength. This gradual build-up of the bound vortex is called the Wagner effect (Berg & Ellington, 1997a; Berg & Ellington, 1997b; Ellington et al., 1996). Depending on the magnitude of the acceleration, it may take up to 6 chord lengths of travel

for the circulation and lift to reach only 90% of the final values (Berg & Ellington, 1997a; Berg & Ellington, 1997b; Ellington et al., 1996). The undulating movements of insect wings make it unlikely that the steady state value is reached at all. Similarly, the chord of a human hand is about 0.1 m, and thus a steady state value of circulation requires about 0.6 m of travel at constant velocity. This makes it unlikely that steady-state circulation is reached at all during the front crawl stroke. Thus, the quasi-steady estimate of lift is overly optimistic, and the discrepancy between calculated and measured forces (Berg & Ellington, 1997a; Berg & Ellington, 1997b; Ellington et al., 1996) becomes even more poignant.

Beneficial unsteady effects have been described as well. The high angles of attack of insect wings during hovering provided a clue. When the angle of attack of a wing exceeds the stall angle, the flow separates and lift force drops dramatically. However, another unsteady effect occurs: flow separation takes time and lift force is in fact briefly increased due to the formation of a leading-edge vortex. This vortex is not bound as in the steady state condition (see Figure 1, right panel), but has its centre of rotation above (and a little bit behind) the leading edge increasing the underpressure on the top surface of the wing. A flow visualisation study with a robotic hawkmoth model, which accurately mimicked the intricate 3-D movements of the real insect wings, revealed the presence of a strong 3-D leading-edge vortex, which could account for 1/3 of the required lift force (Berg & Ellington, 1997a; Berg & Ellington, 1997b; Ellington et al., 1996). This leading-edge vortex was highly unstable for the translating wing in the flowtank. However, the rotational movement of the robotic wing resulted in a strong axial flow component from the base to the tip of the wing, which stabilised the leading-edge vortex. Thus, the wing rotation itself was crucial for stabilising this powerful unsteady lift-enhancing effect.

The overall conclusion of our side step to insect flight is that the quasi-steady approach may fail dramatically in situations where rapid accelerations and decelerations occur. Furthermore, rotations of the moving elements may result in strong 3D flow profiles. Note that in the case of insect hovering the quasi-steady approach is not just somewhat inaccurate, but completely inadequate. Is it appropriate to draw a similar conclusion for the generation of propulsive forces during front crawl swimming?

Kinematic analysis of the trajectory of the hand during the swimming stroke suggests that the hand movements are in fact far from steady, both in terms of velocity and particularly in terms of the direction of movement (Berg & Ellington, 1997a; Berg & Ellington, 1997b; Ellington et al., 1996), while rotations of the arm segments are a prominent feature. Furthermore, a simple hydrodynamic model of the human swimming stroke (a cylinder performing rhythmic rotations about its tip while submerged in a flow tank) showed that for realistic stroke frequencies and fluid speeds the recorded fluid dynamic forces deviated dramatically from the quasi-steady prediction (Berg & Ellington, 1997a; Berg & Ellington, 1997b; Ellington et al., 1996). In view of the above, the validity of the quasi-steady approach of front crawl swimming propulsion can be seriously doubted. Similar to the case of insect flight referred to above, this dilemma can only be resolved by careful analysis of the flow patterns during the stroke, which might, for example, reveal whether the flow around the hand is such that it is indicative for circulation and thus for lift-production. As there is virtually no information regarding the fluid patterns around the arm and hand during swimming, we performed an analysis of the hand and forearm kinematics, while simultaneously recording the flow directions when swimming the front crawl.

METHOD: For a first exploration of the flow around the arm and hand we attached black woollen tufts (Berg & Ellington, 1997a; Berg & Ellington, 1997b; Ellington et al., 1996) to the skin of the left forearm and hand with Leukoplast[®] tape (Beiersdorf AG, Germany). Tufts of about 0.07 m long and 0.02 m apart were attached with tape, which fully surrounded the limb. Such tuft clusters were positioned just below the elbow (10 tufts), halfway the elbow and wrist (10 tufts), at the wrist (8 tufts) and just above the knuckles of the hand (6 tufts only at the back of the hand). Individual tufts were attached to the tip of the thumb (1 tuft), index finger (1 tuft) and little finger (1 tuft). The tufts proved to be clearly visible in most frames, allowing for identification of their free end.

Four competitive swimmers gave informed consent to serve as subjects in this study, which was approved by the local committee on ethics in research on humans. Pulling patterns of the left arm (with tufts) were recorded with 2 gen-locked s-VHS cameras operating at 25 frames per second. The subjects were instructed to swim at a range of speeds (slow, moderate, fast) 3 meters in front of the 'left' camera in the direction of the 'frontal' camera. The s-VHS recordings were synchronised and digitally combined in one frame using Adobe After Effects 3.1. Separate video frames were carefully traced. By comparing consecutive frames the average in-between-frames direction of motion of the index finger tip, the elbow and the shoulder was determined. In this manner, the movement paths of the index finger tip, elbow and shoulder were reconstructed. The displacement from frame to frame gave a rough impression of the velocity, as well (note that effects of perspective were not taken into account). The movement direction of the hand and forearm was determined simultaneously with the flow direction around the limb, as revealed by analysis of the tuft movements.

RESULTS: The flow direction around the hand and arm in relation to the movement direction of the fingertip, elbow and shoulder during a complete stroke is exemplified with data for one subject swimming at a slow pace (about $0.94 \text{ m}\cdot\text{s}^{-1}$). In this recording we captured the complete stroke. All subjects showed similar patterns as presented below. In general, there was an excellent repeatability across trials, particularly for trials of the same subject.

In the glide phase, the arm was kept stretched in front of the gliding swimmer. The fairly stationary tufts during this phase indicate that the flow direction was opposite to the movement direction of the hand and arm.

The insweep phase is characterised by strong elbow flexion and a complete reversal of the flow direction along the hand and arm. The flow direction of each tuft changed rapidly from frame to frame. The direction of the frame to frame changes in tuft orientation generally corresponded to the movement of the forearm and hand.

At the start of the outswEEP an axial flow (directed towards the hand) was present over most of the hand and also started to establish near the elbow. The predominantly axial flow direction at the end of the insweep is not compatible with the concept of circulation around the hand, with associated lift forces.

The outswEEP is the power stroke, characterised by rapid rotation of the whole arm. It is assumed that the largest propulsive forces are generated during this phase. The hand is swept backwards, outwards and upwards with the little finger as the leading edge. A large hand velocity was achieved by the combination of body roll (to the contra-lateral side), retroflexion and abduction of the shoulder and elbow extension (Figure 2). The tufts were neatly arranged and mostly stayed close to the surface of the forearm and hand. Since the tuft orientation with respect to the arm was fairly constant throughout this phase, details of their orientation may be interpreted with confidence. The axial flow component noted earlier stayed very prominent in this phase. The V-shaped convergence of the tufts near the trailing edge of the forearm was observed in 7 consecutive frames (frame 27 – frame 33). This convergence was observed in all subjects, especially during the last part of the outswEEP. This V-shaped convergence of the tufts suggests that the axial flow is accelerating along the arm¹, and that it may be restricted to the 'wake' at the trailing side of the arm (Figure 2, front view of frames 28 and 30). At the wrist the flow split in two paths where part of the tufts (just behind the leading edge) had a proximo-distal axial arrangement along the leading edge, while tufts close to the thumb (trailing edge), as well as those on the fingertips, aligned to the movement direction of the hand. Thus a complex 3-D flow pattern developed around the hand, where at the same instant the flow close to the leading edge had a different direction compared with the flow close to the trailing edge. As flow components perpendicular to the long axis of the arm and hand were almost absent during the outswEEP, circulation and

¹ According to the principle of continuity a fluid column contracts when it accelerates, because its cross-sectional area must always be inversely proportional to its velocity (Berg & Ellington, 1997a; Berg & Ellington, 1997b; Ellington et al., 1996)

associated lift force production may be assumed to be of secondary importance.

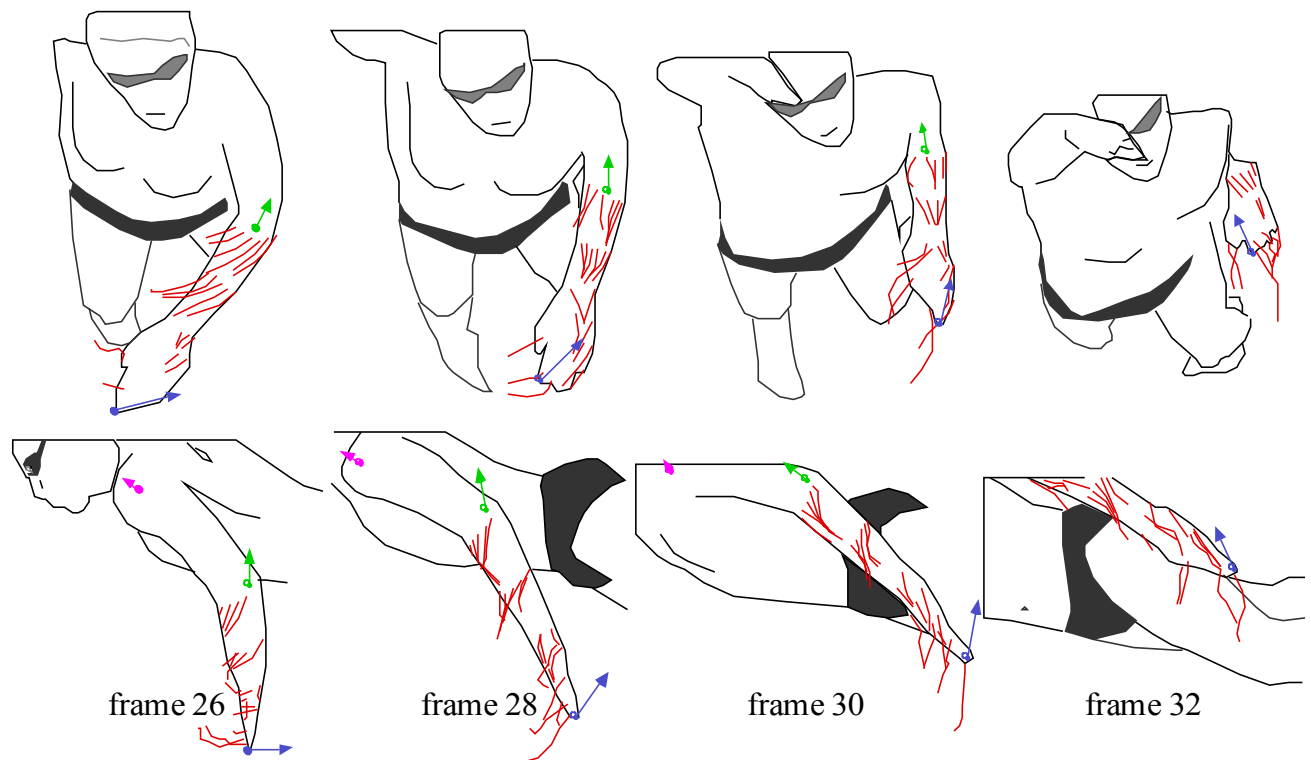


Figure 2 - The latter part of the outswEEP. The movement direction of the fingertip, elbow and shoulder is indicated with arrows.

DISCUSSION: In view of our earlier considerations, such as the Wagner effect and the unpredicted high lift forces generated by an oscillating cylinder (Berg & Ellington, 1997a; Berg & Ellington, 1997b; Ellington et al., 1996), the quasi-steady analysis of front crawl swimming was questioned. The data presented show rapid changes of velocity and direction throughout the insweep and outswEEP and the orientation of the tufts changed virtually from frame to frame, indicating that the flow directions changed rapidly throughout these phases. Furthermore, a strong axial flow component was observed along the arm and hand during the late insweep and throughout the outswEEP. This axial flow is probably associated with the predominantly rotational movement of the arm segments and is not observed in a flowtank set-up. Thus, the quasi-steady analysis must be abandoned.

The present results do not seem to agree with the idea of the hand acting as a lift-producing hydrofoil. During most stages of the stroke the tuft orientation and movements showed that the flow was oriented largely parallel to the long axis of the arm, suggesting that little or no circulation was present around the hand. Only during the early stages of the insweep flow perpendicular to the hand, consistent with circulation, was observed. Therefore, a re-evaluation of the hydromechanic propulsion mechanisms operative during the front crawl swimming is appropriate.

The strong axial flow during the outswEEP was the most striking observation in this study, because this flow component was not in the movement direction of the arm. Throughout the outswEEP, tufts showed a V-shape convergence along the forearm down to the hand, indicating that the axial flow was concentrated at the trailing side of the arm and that this flow was accelerating (see Figure 2). Only very few outswEEP frames showed flow compatible with circulation around the hand. Hence, the generation of lift by the hand seems to play a modest role during the outswEEP. Note that the axial flow components during the inswEEP and outswEEP are associated with rapid rotation of the lower arm and the whole arm, respectively.

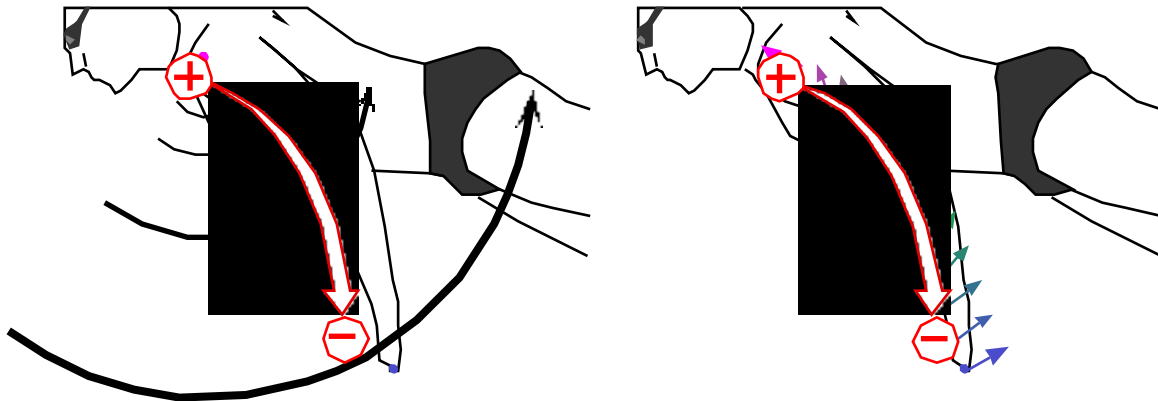


Figure 3 - The rotational movement of the arm during the outswEEP (left frame) creates a velocity gradient along the arm, that, according to Bernoulli's Principle (pressure inversely proportional to velocity), induces a pressure gradient, leading to an axial flow component towards the hand. In the right frame the actual (2-D projected) velocity gradient is shown, including translation of the shoulder due to forward progression and body-roll.

Given these observations, we like to propose a new pumped-up propulsion mechanism for front crawl swimming (Berg & Ellington, 1997a; Berg & Ellington, 1997b; Ellington et al., 1996).

The rotation of the arm during the outswEEP will lead to a velocity gradient along the arm, so that the (tangential) velocity near the hand will be higher than near the elbow. According to Bernoulli's Principle (pressure inversely proportional to velocity), this velocity gradient will create a pressure gradient, where pressure decreases in the direction of the fingertips. This pressure gradient will induce an axial fluid flow along the arm and hand towards the fingertips (see Figs. 2 and 3). The rotating arm acts as a pump, transporting fluid towards the hand.

The next question is how this flow of water is used to generate propulsion. We now will consider three hydrodynamic effects that might contribute to propulsion: 1) the paddling effect in which the hand acts like an oar, 2) an enhanced pressure differential due to the pumping effect, and 3) acceleration of the 'added' mass surrounding the hand and forearm.

We will take as an example data obtained from a recent paper by Berger et al. (Berg & Ellington, 1997a; Berg & Ellington, 1997b; Ellington et al., 1996). In their example the subject swam at $1.3 \text{ m}\cdot\text{s}^{-1}$; since drag related to velocity as $16.4\cdot v^{2.22}$, the average drag at this velocity was 29.5 N. The average hand velocity during the outswEEP was $2.2 \text{ m}\cdot\text{s}^{-1}$, the average hand acceleration $1.75 \text{ m}\cdot\text{s}^{-2}$. It is important to note that, roughly speaking, the hand accelerates throughout the outswEEP up to the last few frames before the hand is pulled out.

Here we will discuss the magnitude of each of the above effects for the outswEEP. Note that probably no propulsion is generated during the glide phase (45% of the stroke cycle) and a limited amount during the inswEEP (10% of the cycle). Hence, we'd expect the mean

propulsive force during the outswEEP (45% of the stroke cycle) to be roughly twice the mean required propulsion for the whole stroke, i.e. roughly 59N. The magnitude of the paddling effect can be estimated with equation 2 (assuming $C_D = 1$, (Berg & Ellington, 1997a; Berg & Ellington, 1997b; Ellington et al., 1996) and a hand plan area of 0.015 m^2) as $0.5 \cdot 1 \cdot 997 \cdot 2.2^2 \cdot 0.015 = 36 \text{ N}$.

The magnitude of the pumping effect may be approximated as follows: The axial flow, with velocity $v_x = 2.2$ (Berg & Ellington, 1997a; Berg & Ellington, 1997b; Ellington et al., 1996) at the back of the hand could enhance the pressure differential across the propelling surface. Assuming no axial flow occurs at the leading edge side of the arm, the effect can be estimated with Bernoulli's equation as $0.5 \cdot 997 \cdot 2.2^2 \cdot 0.015 = 36 \text{ N}$.

The magnitude of the added mass can be estimated using chapter 16 in Vogel (Berg & Ellington, 1997a; Berg & Ellington, 1997b; Ellington et al., 1996). Assuming the forearm and hand to be one cylinder with slenderness ratio 1 yields an added mass coefficient of 1 (Berg & Ellington, 1997a; Berg & Ellington, 1997b; Ellington et al., 1996). The mass of underarm and hand is about $(0.025 \cdot \text{body mass}) = 1.6 \text{ kg}$; the added mass will thus be equal to that. Given the average hand acceleration of $1.75 \text{ m} \cdot \text{s}^{-2}$, the effect of the acceleration of added mass plus hand and forearm will be $3.2 \cdot 1.75 = 5.7 \text{ N}$. The latter calculation excludes the possibility that the axial volume flow of water due to the pumping effect is also involved. In that case the added mass effect would be much stronger.

Simple addition of the paddling-, pumped up and added mass effects yields a propulsive force of 78 N, which is about a third more than the expected value of 59N (of course, the paddling and pumping effects might interact, possibly reducing the total net propulsion). The above simple analysis suggests that in addition to the paddling mechanism (Berg & Ellington, 1997a; Berg & Ellington, 1997b; Ellington et al., 1996), the pumping mechanism could enhance the pressure differential across the propelling surface as well as enlarge the added mass effect and thus account for the observed propulsive forces. However, further study is required to establish the degree of interaction between the proposed mechanisms, which is likely to occur.

The results of this study are reminiscent of studies of insect hovering flight, which demonstrated the failure of the quasi-steady approach and described a strong axial flow component along the rotating wing (Berg & Ellington, 1997a; Berg & Ellington, 1997b; Ellington et al., 1996). Our simple analysis implies that axial flow is a general phenomenon for rotational movements. Therefore, axial flow may also be relevant for the leg kick during swimming, which involves rotations in hip, knee and ankle joints. In fact, in the natural world rotation of propelling elements is very common. Therefore, axial flow may be crucial for understanding propulsion in many other forms of aquatic and aerial locomotion involving rotation of propelling elements, such as fins, paddles, wings and webbed feet.

REFERENCES:

- Berg, C. van den & Ellington, C.P. (1997a). The three-dimensional leading-edge vortex wake of a 'hovering' model hawkmoth. In *Philosophical Transactions of the Royal Society of London* (pp. 329-340). Series B: Biological Sciences 352.
- Berg, C. van den & Ellington, C.P. (1997b). The vortex wake of a 'hovering' model hawkmoth. In *Philosophical Transactions of the Royal Society of London* (pp. 317-328). Series B: Biological Sciences 352.
- Berger, M.A.M., Groot, G. de & Hollander, A.P. (1995). Hydrodynamic drag and lift forces on human hand/arm models. *Journal of Biomechanics*, 28, 125-133.
- Berger, M.A.M., Hollander, A.P. & Groot, G. de (1997). Technique and energy losses in front crawl swimming. *Medicine and Science in Sports and Exercise*, 29, 1491-1498.
- Berger, M.A.M., Hollander, A.P. & Groot, G. de (1999). Determining propulsive force in front crawl swimming: A comparison of two methods. *Journal of Sports Sciences*, 17, 97-105.
- Counsilman, J.E. (1968). *Science of Swimming*. Englewood Cliffs, N.J.: Prentice-Hall.
- Counsilman, J.E. (1971) The application of Bernoulli's principle to human propulsion in water. In L. Lewillie & J.P. Clarys (Eds.), *Swimming I* (pp. 59-71). Brussels: Université Libre de Bruxelles.
- Dickinson, M.H. (1996). Unsteady mechanisms of force generation in aquatic and aerial locomotion. *American Zoologist*, 36, 537-554.

